Long term remediation of highly polluted acid mine drainage: a sustainable approach to restore the environmental quality of the Odiel river basin

Capsule: A high permeable alkaline reactive substrate offers a sustainable option to remediate severely polluted acid mine drainage in the Odiel basin

Manuel A. Caraballo[1*], Francisco Macías[1], Tobias S. Rötting[2], José Miguel Nieto[1] and Carlos Ayora[3].

1 Geology Department, University of Huelva, Campus "El Carmen", E-21071 Huelva, Spain

2 Technical University of Catalonia (UPC), Hydrogeology Group, E-08034 Barcelona, Spain.

3 Institute of Environmental Assessment and Water Research, IDÆA – CSIC, Jordi Girona 18, 08034 Barcelona, Spain.

[*] Corresponding author. Tel.: +34-95-921-9834; fax: +34-95-921-9810

E-mail address: manuel.caraballo@dgeo.uhu.es (Manuel A. Caraballo)

Abstract

During 20 months of proper operation the full scale passive treatment in Mina Esperanza (SW Spain) produced around 100 mg/L of ferric iron in the aeration cascades, removing an average net acidity up to 1,500 mg/L as $CaCO_3$ and not having any significant clogging problem. Complete Al, As, Cd, Cr, Cu, Ti and V removal from the water was accomplished through almost the entire operation time while Fe removal ranged between 170 and 620 mg/L. The system operated at a mean inflow rate of 43 m^3/day achieving an acid load reduction of 597 $g \cdot (m^2 \cdot day)^{-1}$, more than 10 times higher than the generally accepted 40 $g \cdot (m^2 \cdot day)^{-1}$ value commonly used as a passive treatment system designing criteria. The high performance achieved by the passive treatment system at Mina Esperanza demonstrates that this innovative treatment design is a simple, efficient and long lasting remediation option to treat highly polluted acid mine drainage.

Keywords

Acid mine drainage, passive treatment system, Iberian Pyrite Belt, schwertmannite, hydrobasaluminite

1. Introduction

Acid mine drainage (AMD) generation has been thoroughly described in many previous studies related with inorganic water pollution (Bigham and Nordstrom, 2000; Younger et al., 2002). It is sufficient here to state that it arises from the oxidative dissolution of sulfide minerals, mainly pyrite, ordinarily present as main ore-forming minerals in sulfide mining districts (Akcil and Koldas, 2006) or as minor constituents in coal deposits (Younger et al., 2002).

About 19,300 km of rivers and streams and more than 72,000 ha of lakes and reservoirs in the continental USA have been damaged by AMD (Kleinmann, 1989). In England and Wales, it is estimated that some 1,800 km of surface streams and rivers are currently impacted by AMD (Jarvis et al., 2006), whereas in SW Spain, from a total of 1,149 km of the river network examined at the Odiel basin, 427 km were affected by AMD (Sarmiento et al., 2009b). These studies clearly present AMD water pollution as a widespread and intense environmental problem that, taking into account only three countries in the world, implies more than 21,500 km of rivers and streams affected.

The Iberian Pyrite Belt (IPB), located in the south-west of the Iberian Peninsula, can be considered one of the biggest massive sulfide deposits in the world with a length of over 200 km, a width of about 40 km and original estimated reserves in the order of 1,700 Mt of sulfide ore (Sáez et al., 1999). The result of the intense mining during almost 5,000 years (Leblanc et al., 2000) is a region where abandoned sulfide-rich wastes in spoil heaps and tailings and flooded underground mines and opened pits generate an ubiquitous problem of AMD pollution (Achterberget al., 2003; Sarmiento et al., 2009a).

As the main economic activity in the Huelva province (IPB) has changed from mining to agriculture, the current pollution and possible remediation of inland water resources in the Odiel river basin has become an issue of great concern.

AMD can be remediated by two generic approaches: active or passive treatment. While the former is more appropriate to be used in mines under operation where fast remediation of enormous amounts of water is needed, the latter is a more realistic solution when AMD remediation has to be achieved in abandoned mine sites (like the ones at the IPB) where the absence of any accountable entity and the remote location

require the use of a long lasting, low cost and environmentally sustainable treatment option with no artificial energy requirements (PIRAMID-Consortium, 2003).

Traditional sulfate reducing bacteria (SRB) based treatments, like anaerobic wetlands (Kröpfelová et al., 2009; Marchand et al., 2010) or reactive permeable barriers (Jarvis et al., 2006; Caraballo et al., 2010), have shown encouraging results treating AMD at coal mining districts, however they are not very useful to treat highly polluted AMD in areas with limited available space because SRB have maximum tolerance levels for certain metals and need a high residence time, up to six days (Neculita et al., 2008), to achieve an optimal bacterial growth. Limestone based treatments like anoxic limestone drainages (Santomartino and Webb, 2007) or limestone sand reactors (Watten et al., 2005) although efficient at treating AMD with low to moderate metal concentrations, commonly exhibit serious problems of clogging and passivation when exposed to AMD with high metal concentrations.

To overcome all the problems shown by the typical passive treatment systems treating highly polluted AMD and design a treatment to be implemented in the IPB, Rötting et al. (2008b) developed the dispersed alkaline substrate (DAS), consisting of a reactive mixture of pine wood shavings and limestone sand. The high metal removal performance of this reactive mixture has been broadly tested both in laboratory columns (Rötting et al., 2008b) and field-scale experiments (Rötting et al., 2008a; Caraballo et al., 2009a) for the highly polluted AMD at the IPB.

The main scope of the present study is to show the encouraging results obtained after 20 months of continuous operation of the full-scale DAS passive treatment system implemented at Mina Esperanza and offer this technology as a environmentally and economically sustainable treatment option for a future complete remediation of river basins affected by highly polluted AMD. Water chemistry, precipitate mineralogy and

metal removal efficiency of the different sections comprising the treatment will be presented to gain a better understanding of the different hydrochemical, mineralogical and operational processes involved in AMD remediation.

2. Methods and sampling procedure

2.1. Site location

Mina Esperanza is located in the northern part of the IPB (Fig. 1A), in South-western Spain (37º45´34´´N-6º41´00´´O). The mineralization at Mina Esperanza consists of a massive pyrite deposit with minor amounts of chalcopyrite (Pinedo-Vara, 1963). The country rocks are slates and low grade metamorphic phyllites. The AMD emerging from the adit is channeled by a creek, known as Esperanza creek, for 1 km to the Odiel River and can be considered one of the first important pollution sources to this river in the upper section of its basin (Sarmiento et al. 2009b).

AMD composition at the exit of the adit and the main hydrochemical parameters are shown in Table 1.

2.2. Water sampling

Water samples were taken at least twice a month from March 2007 to October 2008, a total of 42 sampling campaigns along the 20 months of the system operation time. Six sampling points were selected as representative of the different sections of the treatment system (Fig. 1A) and called: Adit, T-in (reactive tank input), T-sup (reactive tank supernatant), T-out (reactive tank output), D-in (decantation pond input) and D-out (decantation pond output). Water samples were filtered immediately after collection through 0.1 µm Millipore filters on Millipore syringe filter holders, acidified in the field to pH < 1 with suprapur HNO_3 and stored at 4 ºC in 60 mL sterile polypropylene containers until analyzed.

111 *2.3.* Field in-situ measurements

112 Temperature and electrical conductivity were measured using a portable CM35 meter
113 (Crison®) with 3 point calibration (147 and 1413 µS/cm and 12.88 mS/cm). The pH and
114 redox potential were measured using a PH25 meter (Crison®) with Crison electrodes.
115 Redox potential and pH were controlled and calibrated using 2 points (240–470 mV)
116 and 3 points (pH 4.01–7.00–9.21), respectively, with Crison standard solutions. Redox
117 potential measurements were corrected to the Standard Hydrogen Electrode to calculate
118 pe. Dissolved O_2 was measured with an auto-calibrating Hanna® portable meter and
119 gross alkalinity was determined using CHEMetrics® Total Titrets® (range 10–100 or
120 100–1,000 mg/L as $CaCO_3$ equivalents, accuracy approximately 5%).

121 *2.4.* Laboratory analytical techniques

122 Concentrations of dissolved Al, As, Ba, Be, Ca, Cd, Co, Cr, Cu, Fe, K, Li, Mg, Mn,
123 Na, Ni, S, Si, Sr, Ti, V and Zn were determined by Inductively Coupled Plasma Atomic
124 Emission Spectrometry (ICP-AES Jobin- Ybon Ultima2) using a protocol especially
125 designed for AMD samples (Tyler et al., 2004). Analysis was performed at the Central
126 Research Services of the University of Huelva. Multielement standard solutions
127 prepared from single certified standards supplied by SCP SCIENCE were used for
128 calibration. They were run at the beginning and at the end of each analytical series.
129 Certified Reference Material SRM-1640 NIST fresh-water-type and inter-laboratory
130 standard IRMM-N3 wastewater test material (European Commission Institute for
131 Reference Materials and Measurements) were also analyzed. Detection limits were
132 calculated by average and standard deviations from 10 blanks. Detection limits were:
133 200 µg/L for Al, Fe, Mn, Mg, Na, K, Si and S; 500 µg/L for Ca; 50 µg/L for Zn; 5 µg/L
134 for Cu; 2 µg/L for As and 1 µg/L for the other trace elements.

Net acidity (Ac) (mg/L as $CaCO_3$ equivalents) was calculated using the following equation after Rötting et al., 2008a:

$$Ac = 50{,}045 \cdot (3 \cdot c_{Al} + 2 \cdot c_{Fe} + 2 \cdot c_{Mn} + 2 \cdot c_{Zn} + 10^{-pH}) - alk \quad (1)$$

where c_X are molar concentrations of the different metals (mol/L) and alk is measured gross alkalinity (mg/L as $CaCO_3$ equivalents).

Relative metal removal r (%) at the output of the system was calculated as:

$$r = \frac{(c_{in} - c_{out})}{c_{in}} \cdot 100 \quad (2)$$

where c_{in} is the adit concentration (mg/L) and c_{out} is the concentration at the output (D-out) of the system (mg/L).

Acid load reduction RA (g/(m^2 · day)), normalized by system area was calculated as:

$$RA = Q \cdot \frac{Ac_{in} - Ac_{out}}{1{,}000 \cdot A} \quad (4)$$

where Q is flow rate (m^3/day), Ac_{in} and Ac_{out} are adit and system's outflow net acidity (mg/L as $CaCO_3$ equivalents), respectively, and A is horizontal area of the treatment system (m^2).

3. Treatment concept and design

A concrete opened channel was built to direct the AMD emerging from the adit to the reactive tank. To improve AMD oxygenation a five-step cascade was included in the mid-section of the opened channel (Fig. 1A).

The reactive tank was filled with a 2.5 m layer of limestone-DAS, 80% v/v pine wood shavings and 20% v/v limestone sand. This reactive material has a high porosity (50%) that is essential to maintain its hydraulic conductivity and to minimize the clogging problems suffered by passive treatment systems precipitating solids within the

156 porous space of the reactive material. At the bottom of the reactive material, a 50 cm
157 drain layer of coarse quartz gravel was placed (Fig. 1B). Water flow through the
158 reactive material was gravity forced from top to bottom, finally emerging from the top
159 of the water collecting well, creating an initial supernatant depth of 25 cm and a
160 freeboard of 1 m (Fig. 1B). The residence time for the AMD within the reactive
161 material typically ranged from 2.5 to 5 days for common inflow rates ranging from 86
162 to 43 m^3/day.

163 The third and final step of the treatment system is a 90 m^3 decantation pond. This
164 section was connected with the reactive tank by the use of a concrete opened channel in
165 the form of a three steps aeration cascade (Fig. 1A). The high volume of the pond
166 implies a residence time for the AMD of 2.25 days if a 43 m^3/day inflow is considered.

167 **4. Results and discussion: Mina Esperanza performance**

168 *4.1.* Water chemistry evolution throughout the treatment

169 The treatment system can be conceptually divided into four main sections: first
170 oxidation cascades, reactive tank, second oxidation cascades and decantation pond (Fig.
171 1A). To achieve a better understanding of the role played by each section in the overall
172 system performance and for the sake of simplicity, time evolution for only two
173 physical-chemical parameters (pH and pe), one operational parameter (flow rate),
174 concentration of five major elements (Al, Ca, Cu, Fe and Si), as well as alkalinity and
175 net acidity, will be presented (Fig. 2 and 3). This section will show an overview of the
176 different processes taking place in the system while the time evolution of the selected
177 parameters of the system will be shown in the following section.

178 A significant pe increase can be observed in the AMD after flowing along the
179 aeration cascades, remaining around the same value at the supernatant check point (Fig.

2). This pe increase and the linked oxidation of around 100 mg/L of ferrous to ferric iron in the AMD (data not shown) was probably related to the presence of a particular community of algae and bacteria developed on the surface of the open channels. These microorganisms and their exact roles are currently being studied in detail.

As expected, flow of AMD through the reactive tank caused the main hydrochemical changes along the treatment. From the input to the output of the reactive tank, the water pH increased from <3 to a value around 6.5 while a coupled inverse behavior was showed by pe values (Fig. 2). Calcite dissolution within the reactive tank can distinctly be observed in the significant increase in Ca concentration (Fig. 3) and alkalinity (Fig. 2) in the waters flowing out of the reactive tank. This pH increase induces Fe precipitation and complete Al removal (Fig. 3) within the reactive tank, as well as total Cu removal and a significant Si depletion in the AMD (Fig. 3). The processes of Fe and Al precipitation and coprecipitation and/or adsorption of other metals have been widely studied in many laboratory and field experiments using limestone-DAS to remediate AMD (Rötting et al., 2008a; Caraballo et al., 2009a; Caraballo et al., 2009b) and the reader is referred to these works for further details. The primary role of the reactive tank in the whole treatment performance is demonstrated by the achievement of a net acidity removal within the reactive mixture in the range of 1,500 mg/L as $CaCO_3$ equivalents (Fig. 3).

Although comparison of T-out and D-in waters show an almost negligible change in water pe and a very small increase in ferric iron (Fig. 2), it is important to notice that both the water iron removal and the remarkable amount of Fe(III) precipitates formed along the channel suggest a noticeable ferric iron generation. This situation can be explained by the significant increase of iron abiotic oxidation at circumneutral pH

values and the coupled rapid precipitation of goethite in these special water conditions (Bigham and Nordstrom, 2000).

A significant iron removal (Fig. 3) and alkalinity consumption (Fig. 2) was achieved in the decantation pond. While iron precipitation tends to lower water pH by the generation of H^+ (Bigham and Nordstrom, 2000), this effect is counteracted by the remarkable alkalinity of the DAS-treated water leading to a final water pH close to the value observed at the reactive tank output.

4.2. Time evolution of the treatment's performance and metal removal

Throughout most of the first year of operation the hydrochemical behavior of the system was quite steady, however after this period some slight changes were observed in the reactive tank and subsequently in the decantation pond. A slow decrease in water pH at the reactive tank output was observed during the last eight months of operation (Fig. 2). This pH time evolution from 6.0 in March 2008 to 5.1 in October 2008 was associated with a progressive decrease in water alkalinity from 200 mg/L as $CaCO_3$ to close to 0 mg/L as $CaCO_3$ for the same period of time (Fig.2). In addition to this effect and connected to the alkalinity decrease at the reactive tank output, an important decrease in the pH at the decantation pond output was observed (Fig. 2).

Aluminum, copper and cadmium were completely removed within the reactive tank during the first year of operation, showing only a slight decrease in the relative removal of these elements during the last months of operation (Fig. 4). Aluminum was the least sensitive of these three elements to the observed water pH change and only when water pH was close to 5 a very small decrease in aluminum removal was observed (Fig. 4). This observation is in accordance with the proposed pH value of 5 for hydrobasaluminite ($Al_4(SO_4)(OH)_{10}\cdot 15H_2O$) precipitation in AMD (Bigham and Nordstrom, 2000). The more pronounced effect that water pH decrease had on Cu and

Cd relative removal (Fig. 4) is in agreement with the hypothesis of pH dependent adsorption as the most likely removal process for these two elements, as shown in previous DAS field experiments (Caraballo et al., 2009a). Iron removal during the great majority of the treatment's operation time ranged between 20% and 40% and was not clearly affected by decreases in pH and alkalinity during the last months of operation (Fig.4). A complete removal for As, Cr, Ti and V was observed throughout the entire operation time of the treatment system (Fig. 4). Arsenic removal coupled to iron precipitation has been previously reported for DAS-based passive treatment systems (Caraballo et al., 2009a) as well as for natural environments (Asta et al., 2009).

Unexpectedly low pe values, ranging from 1.5 to 3, during the first months of operation, followed by a dramatic water pe increase with time was observed in the reactive tank outflow (Fig. 2). In addition, a very high Zn, Co and Ni relative removal was achieved for the six first months of operation (Fig. 4). After some months, the initial important metal removal for these elements progressively decreased leading to a negative metal removal (output water concentration higher than input water concentration) that was clearly correlated with the water pe increase (Fig. 4). Chemically induced Zn, Co and Ni precipitation as hydroxides can only be expected after reaching a pH value higher than 8, 9 and 10 respectively (Rötting et al., 2008c). The presence of organic matter (wood shavings) in the reactive material and the two months that the reactive tank remained flooded previous to the system inauguration could have facilitated the growth of some sulfate reducing bacteria (SRB) within the reactive mixture, thus offering a possible explanation for the remarkable Zn, Co and Ni removal during the first months of operation. However due to the high flow rate employed in the treatment and the subsequent low residence time within the reactive mixture, the environmental conditions were no longer favorable for the optimal growth

254 of SRB and therefore it could be implied that the activity of these bacteria progressively
255 ceased, and subsequently the removal of Zn, Co and Ni ceased as well.

256 *4.2.* System efficiency

257 To have a better understanding of the high pollution that the treatment at Mina
258 Esperanza has to accommodate, and the high remediation efficiency achieved by the
259 treatment, it was decided to compare the 42 sampling campaigns from Mina Esperanza
260 with the available data of 83 different passive treatment systems recapped for the USA
261 by Ziemkiewicz et al. (2003). This study comprised 11 anaerobic wetlands (AnW), 28
262 anoxic limestone drains (ALD), 16 vertical flow wetlands (VFW), 10 oxic limestone
263 channels (OLC) and 18 limestone leach beds (LSB).

264 Inflow net acidity was calculated to offer an estimation of the metal pollution to
265 which each passive treatment system was subjected. As shown in the top of figure 5A,
266 net acidity achieved a median value as high as 2,300 mg/L as $CaCO_3$ for the treatment
267 at Mina Esperanza (ME). It can also be noticed that the inflow net acidity at ME is
268 typically one order of magnitude higher than the median value exhibited by the great
269 majority of the treatments compared in this section.

270 To compare the removal capacity of the different treatments, it was decided to
271 employed the net acidity removal because this parameter offers a good approach to the
272 acidity neutralization capacity of the treatments and also to the amount of metal
273 removed (according to equation 1). Net acidity removal was calculated by subtracting
274 the net acidity at the system output to the inflow net acidity. Median net acidity removal
275 achieved in ME was observed to be 5 times higher than the same value for VFW and
276 ALD, up to 15 times higher than the median values achieved in AnW and LSB and as
277 much as 43 times higher comparing with LSB (Fig. 5A bottom). It can also be observed
278 that the third quartile for ME is considerably broader than the first quartile, implying

279 that changes in net acidity removal for ME typically moves to achieved higher values
280 close to 2,000 mg/L as $CaCO_3$.

281 Acid load reduction in $g\cdot(m^2\cdot day)^{-1}$ is a parameter commonly employed to
282 characterize the surface efficiency of a passive treatment system and therefore can be
283 used to gain a better understanding of the surface land requirement of the different
284 passive treatments. Comparing the available median values for AnW and VFW with the
285 values obtained for ME it can be observed that the median removal efficiency achieved
286 in ME (597 $g\cdot(m^2\cdot day)^{-1}$) is 32 times higher than the median values obtained for the
287 AnW and as much as 47 times higher compared with VFW median values (Fig. 5B).
288 This observation has to be seriously taken into account when choosing a remediation
289 option for a site for cases in which the land to build a passive treatment system is scarce
290 and/or expensive. On the other hand, when land availability is not an important
291 influence on the project budget, the construction of a passive treatment system
292 achieving, for instance, the same acid load reduction as observed at ME (with a surface
293 area of 120 m^2) would require the use of more than 3,600 m^2 in the best case and up to
294 5,600 m^2 for the worst scenario. The large land requirements of the other treatment
295 methods would have a clear visual and environmental impact in the landscape of any
296 region and even more important it drastically increases the construction cost of the
297 passive treatment system. The results obtained at ME (in term of acid load reduction)
298 improve by more than 10 times the generally accepted 40 $g\cdot(m^2\cdot day)^{-1}$ values developed
299 by the U.S. Bureau of Mines (Hedin et al., 1994) and commonly used as a system
300 designing criterion.

301 **5. Conclusions**

302 The passive treatment system implemented in Mina Esperanza offers a good example
303 of a simple design overcoming the most typical operational problems suffered by

304 traditional passive treatment systems when they are exposed to highly metal polluted
305 waters. The high porosity and hydraulic conductivity showed by the limestone-DAS
306 reactive material enabled the system to treat a high inflow (ranging between 43 and 86
307 m^3/day) for 20 months without suffering any significant clogging problem.

308 During its long operation time the system achieved a high and consistent metal
309 removal with mean removal values of 144 ± 9 mg/L Al, 16 ± 6 mg/L Cu, 40 ± 4 mg/L
310 Si, 490 ± 75 µg/L As, 73 ± 9 µg/L Cd, 28 ± 6 µg/L Cr, 85 ± 50 µg/L Ni, 10 ± 3 µg/L Ti
311 and 94 ± 18 µg/L V. Iron was the main removed metal in the system ranging from 170
312 to 620 mg/L depending on the system performance. However, after one year of
313 operation the system showed a slight decrease on Al, Cu and Cd removal due to
314 limestone depletion in the reactive material and subsequent pH and alkalinity
315 decrement.

316 The high efficiency attained by the passive treatment system was illustrated by the
317 high inflow net acidity and the significant net acidity removed from the treated AMD.
318 These two parameters showed to be typically one order of magnitude higher than the
319 values reported for more than 80 traditional passive treatment systems in the USA.
320 Furthermore, the high acid load reduction, expressed in terms of $g\cdot(m^2\cdot day)^{-1}$, reached
321 by the treatment at Mina Esperanza was 10 times higher than the generally accepted 40
322 $g\cdot(m^2\cdot day)^{-1}$ value commonly used as a passive treatment system designing criteria.

323 All these observations have important implications for the future design of complete
324 passive treatment systems to be exposed to highly polluted AMD, and their future
325 implementation in new remediation sites at the Odiel basin should be seriously
326 considered as an efficient and economic way of remediating the environmental
327 problems suffered by the waters of this region. To this end, a complete full scale passive
328 treatment system is under construction in Mina Esperanza. This new system (estimated

329 costs of 300,000-500,000€) will comprise 3 limestone-DAS reactive tanks alternating 6
330 decantation ponds allowing to treat up to 2.5 L/s of highly polluted AMD. These
331 treatment improvements will address some of the problems observed on the present
332 experiment, namely: incomplete Fe removal from the water, Al-Cu-Cd incomplete
333 water removal after one year of operation and low water pH and alkalinity concentration
334 at the output of the treatment.

335 **Acknowledgments**

336 We are grateful to Rich B. Wanty from U.S. Geological Survey for all the corrections
337 and suggestions improving the quality of this paper. This study was funded by the
338 Spanish Ministry of Science and Technology through project CTM2007-66724-
339 C02/TECNO and by the Environmental Council of the Andalusia Regional
340 Government. M.A.C. was financially supported by the Spanish Government with a FPU
341 PhD fellowship. We would also like to thank Professor William J. Manning (Editor-in-
342 Chief) and two anonymous reviewers for their comments that significantly improved the
343 quality of this paper.

344 **References**

345 Achterberg, E.P., Herzl, V.M.C., Braungardt, C.B., Millward, G.E., 2003. Metal
346 behaviour in an estuary polluted by acid mine drainage: the role of particulate matter.
347 Environmental Pollution 121, 283-292.

348 Akcil, A., Koldas, S., 2006. Acid Mine Drainage (AMD): causes, treatment and case
349 studies. Journal of Cleaner Production 14, 1139-1145.

350 Asta, M.P., Ayora, C., Román-Ross, G., Cama, J., Acero, P., Gault, A.G., Charnock,
351 J.M., Bardelli, F., 2009. Natural attenuation of arsenic in the Tinto Santa Rosa acid
352 stream (Iberian Pyritic Belt, SW Spain): The role of iron precipitates. Chemical
353 Geology 271, 1-12.

354 Bigham, J.M., Nordstrom, D.K., 2000. Iron and Aluminum Hydroxysulfates from
355 Acid Sulfate Waters. In: Alpers, C.N., Jambor, J.L., Nordstrom, D.K. eds.), Sulfate
356 Minerals: Crystallography, Geochemistry, and Environmental Significance. Reviews in
357 Mineralogy and Geochemistry, Mineralogical Society of America., Chantilly, Virginia,
358 351-403.
359 Caraballo, M.A., Rötting, T.S., Macías, F., Nieto, J.M., Ayora, C., 2009a. Field
360 multi-step limestone and MgO passive system to treat acid mine drainage with high
361 metal concentrations. Applied Geochemistry 24, 2301-2311.
362 Caraballo, M.A., Rotting, T.S., Nieto, J.M., Ayora, C., 2009b. Sequential extraction
363 and DXRD applicability to poorly crystalline Fe- and Al-phase characterization from an
364 acid mine water passive remediation system. American Mineralogist 94, 1029-1038.
365 Caraballo, M.A., Santofimia, E., Jarvis, P.A., 2010. Metal retention, mineralogy and
366 design considerations of a mature Permeable Reactive Barrier (PRB) for acidic mine
367 water drainage in Northumberland, UK. American Mineralogist 95, 1642-1649.
368 Hedin, R.S., Nairn, R.W., Kleinmann, R.L.P., 1994. Passive treatment of coal mine
369 drainage. US Bureau of Mines IC9389, Pittsburgh, PA, USA.
370 Jarvis, A.P., Moustafa, M., Orme, P.H.A., Younger, P.L., 2006. Effective remediation
371 of grossly polluted acidic, and metal-rich, spoil heap drainage using a novel, low-cost,
372 permeable reactive barrier in Northumberland, UK. Environmental Pollution 143, 261-
373 268.
374 Kleinmann, R.L.P. 1989. Acid mine drainage in the United States controlling the
375 impact on streams and rivers. In: 4th World Congress on the Conservation of the Built
376 and Natural Environments, University of Toronto, 1–10.

377 Kröpfelová, L., Vymazal, J., Svehla, J., Stíchová, J., 2009. Removal of trace elements
378 in three horizontal sub-surface flow constructed wetlands in the Czech Republic.
379 Environmental Pollution 157, 1186-1194.
380 Leblanc, M., Morales, J.A., Borrego, J., Elbaz-Poulichet, F., 2000. 4,500 year old
381 mining pollution in southwestern Spain: long term implications for modern mining
382 pollution. Economic Geology 95, 655-662.
383 Marchand, L., Mench, M., Jacob, D.L., Otte, M.L., 2010. Metal and metalloid
384 removal in constructed wetlands, with emphasis on the importance of plants and
385 standardized measurements: A review. Environmental Pollution 158, 3447-3461.
386 Neculita, C.M., Zagury, G.J., Bussière, B., 2008. Effectiveness of sulfate-reducing
387 passive bioreactors for treating highly contaminated acid mine drainage: II. Metal
388 removal mechanisms and potential mobility. Applied Geochemistry 23, 3545–3560.
389 Pinedo-Vara, I., Piritas de Huelva. Su historia, minería y aprovechamiento. Summa,
390 Madrid, Spain, 1963.
391 PIRAMID-Consortium. Engineering guidelines for the passive remediation of acidic
392 and/or metalliferous mine drainage and similar wastewaters. University of Newcastle,
393 Newcastle Upon Tyne, UK, 2003.
394 Rötting, T.S., Caraballo, M.A., Serrano, J.A., Ayora, C., Carrera, J., 2008a. Field
395 application of calcite Dispersed Alkaline Substrate (calcite-DAS) for passive treatment
396 of acid mine drainage with high Al and metal concentrations. Applied Geochemistry 23,
397 1660-1674.
398 Rötting, T.S., Thomas, R.C., Ayora, C., Carrera, J., 2008b. Passive treatment of acid
399 mine drainage with high metal concentrations using dispersed alkaline substrate. Journal
400 of Environmental Quality 37, 1741-1751.

401 Rötting, T.S., Ayora, C., Carrera, J., 2008c. Improved passive treatment of high Zn
402 and Mn concentrations using Caustic Magnesia (MgO): Particle size effects.
403 Environmental Science and Technology 24, 9370–9377.
404 Sáez, R., Pascual, E., Toscano, M., Almodóvar, G.R., 1999. The Iberian type of
405 volcano-sedimentary massive sulphide deposits. Mineralium Deposita 34, 549-570.
406 Santomartino, S., Webb, J.A., 2007. Estimating the longevity of limestone drains in
407 treating acid mine drainage containing high concentrations of iron. Applied
408 Geochemistry 22, 2344-2361.
409 Sarmiento, A.M., Nieto, J.M., Casiot, C., Elbaz-Poulichet, F., Egal, M., 2009a.
410 Inorganic arsenic speciation at river basin scales: The Tinto and Odiel Rivers in the
411 Iberian Pyrite Belt, SW Spain. Environmental Pollution 157, 1202-1209.
412 Sarmiento, A.M., Nieto, J.M., Olías, M., Cánovas, C.R., 2009b. Hydrochemical
413 characteristics and seasonal influence on the pollution by acid mine drainage in the
414 Odiel river Basin (SW Spain). Applied Geochemistry 24, 697-714.
415 Tyler, G., Carrasco, R., Nieto, J.M., Perez, R., Ruiz, M.J., Sarmiento, A.M., 2004.
416 Optimization of Mayor and Trace Element Determination on Acid Mine Drainage
417 samples by Ultrasonic Nebulizer-ICP-OES (USN-ICP-OES) Pittcon Conf. 7–12 March.
418 Chicago, USA.
419 Watten, B.J., Sibrell, P.L., Schwartz, M.F., 2005. Acid neutralization within
420 limestone sand reactors receiving coal mine drainage. Environmental Pollution 137,
421 295-304.
422 Younger, P.L., Banwart, S.A., Hedin, R.S., 2002. Mine Water: Hydrology, Pollution,
423 Remediation. Kluwer Academic Publishers, Dordrecht.

Ziemkiewicz, P.F., Skousen, J.G., Simmons, J., 2003. Long-term Performance of Passive Acid Mine Drainage Treatment Systems. Mine Water and the Environment 22, 118-129.

FIGURE CAPTIONS

Figure 1. A) Location and schematic plan view of the passive treatment at Mina Esperanza. 1 = Adit, 2 = reactive tank input, 3 = reactive tank supernatant, 4 = reactive tank output, 5 = decantation pond input and 6 = decantation pond output. B) Schematic cross section of the reactive tank.

Figure 2. Time evolution for pH, pe, alkalinity and flow rate at the six check points in the passive treatment system. T-in = reactive tank input, T-sup = reactive tank supernatant, T-out = reactive tank output, D-in = decantation pond input and D-out = decantation pond output. Note: Alkalinity was zero throughout the entire study in Adit, T-in and T-sup.

Figure 3. Box and whisker diagrams for the most significant major metals and net acidity. Minimum, first quartile, median, third quartile and maximum values are shown for the six check points in the passive treatment system.

Figure 4. Time evolution of metal relative removal (%) achieved by the system from the adit to the outflow of the decantation pond. pH and pe values are plotted to compare the effect of these factors on the removal of certain metals.

Figure 5. A) Box and whisker diagrams comparing inflow net acidity and net acidity removal, and B) acid load reduction values for Mina Esperanza and more than 80 traditional passive treatment systems at the USA. AnW = anaerobic wetland, VFW = vertical flow wetland, ALD = anoxic limestone drains, OLC = opened limestone channels, LSB = limestone leach beds and ME = Mina Esperanza.

TABLES

449 Table1. AMD composition and physico-chemical parameters at the adit.

Table

Table1. AMD composition and physico-chemical parameters at the adit

Major elements (mg/L)										
Al	Ca	Cu	Fe	K	Mg	Mn	Na	SO_4^{2-}	Si	Zn
128-167	146-194	12-24	755-1,100	5-34	149-215	4-6	21-26	3,324-4,515	44-60	19-33
Minor elements (µg/L)										
As	Ba	Be	Cd	Co	Cr	Li	Ni	Sr	Ti	V
357-692	4-6.5	4-10	66-98	468-759	22-42	138-381	152-247	131-189	6.5-15	84-129
Physical-chemical parameters										
pH	Eh	Conductivity (mS/cm		T (ºC)	Dissolved Oxygen (mg/L)			Dissolved oxygen (%)		
2.35-2.96	555-597	3.24-6.12		16.8-22.2	1.8-2.5			13-28		

Minimum and maximum values obtained in the 42 sampling campaigns (March 2007-October 2008)

Figure

Fig. 1

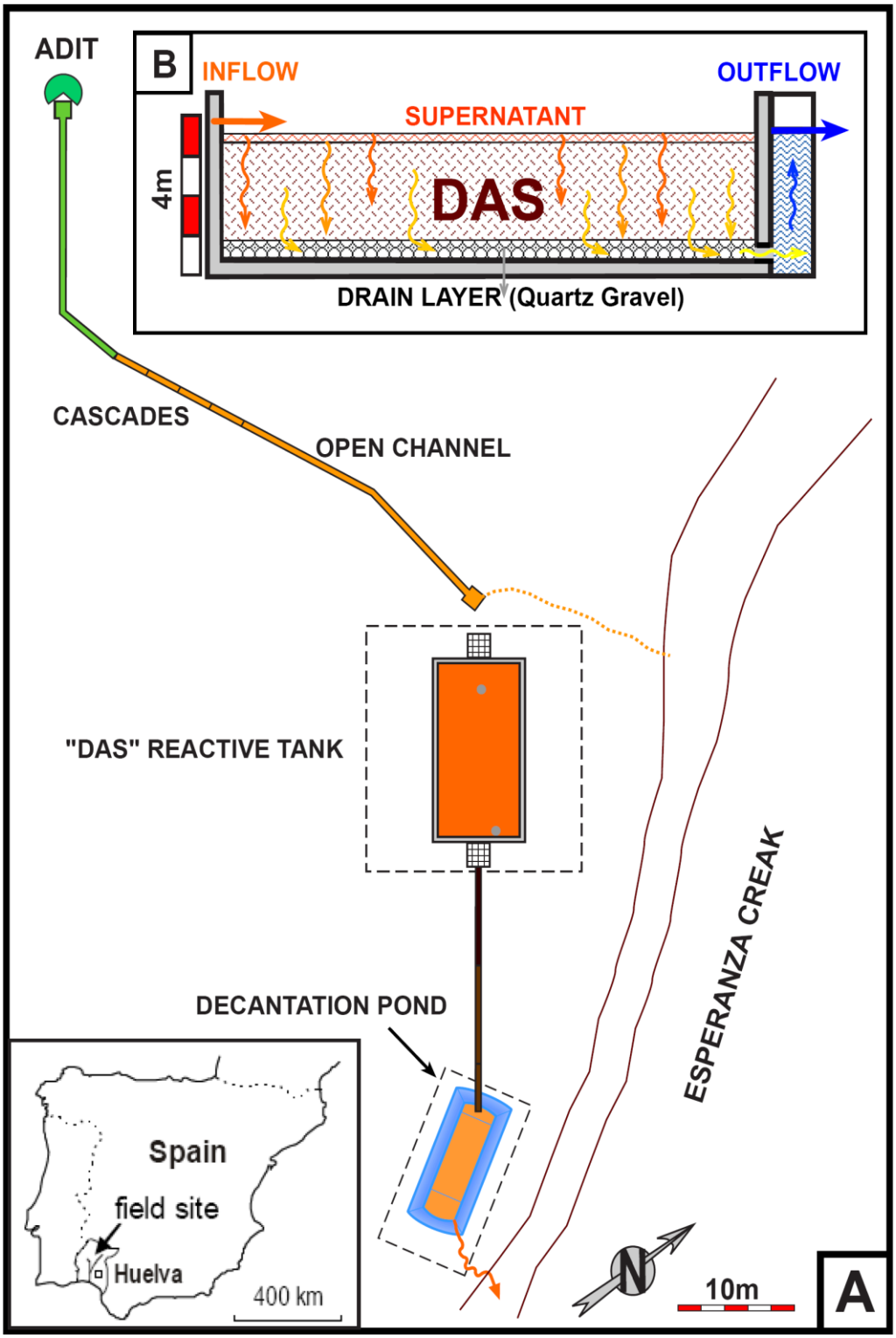
ADIT
B
INFLOW
OUTFLOW
SUPERNATANT
4m
DAS
DRAIN LAYER (Quartz Gravel)
CASCADES
OPEN CHANNEL
"DAS" REACTIVE TANK
DECANTATION POND
ESPERANZA CREAK
Spain
field site
Huelva
400 km
N
10m
A

Figure

Fig. 2

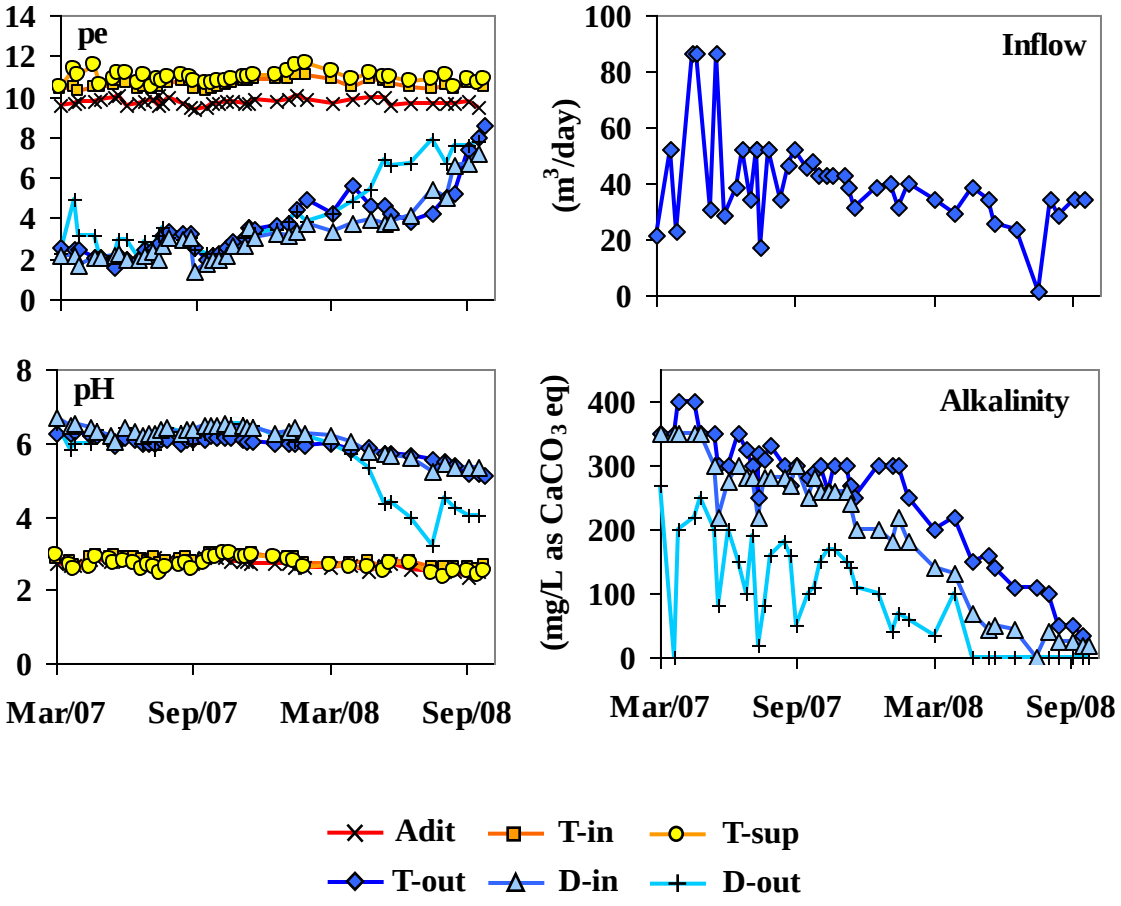
pe
Inflow
pH
Alkalinity
(m3/day)
(mg/L as CaCO3 eq)
Mar/07
Sep/07
Mar/08
Sep/08
Adit
T-in
T-sup
T-out
D-in
D-out

Figure

Fig. 3

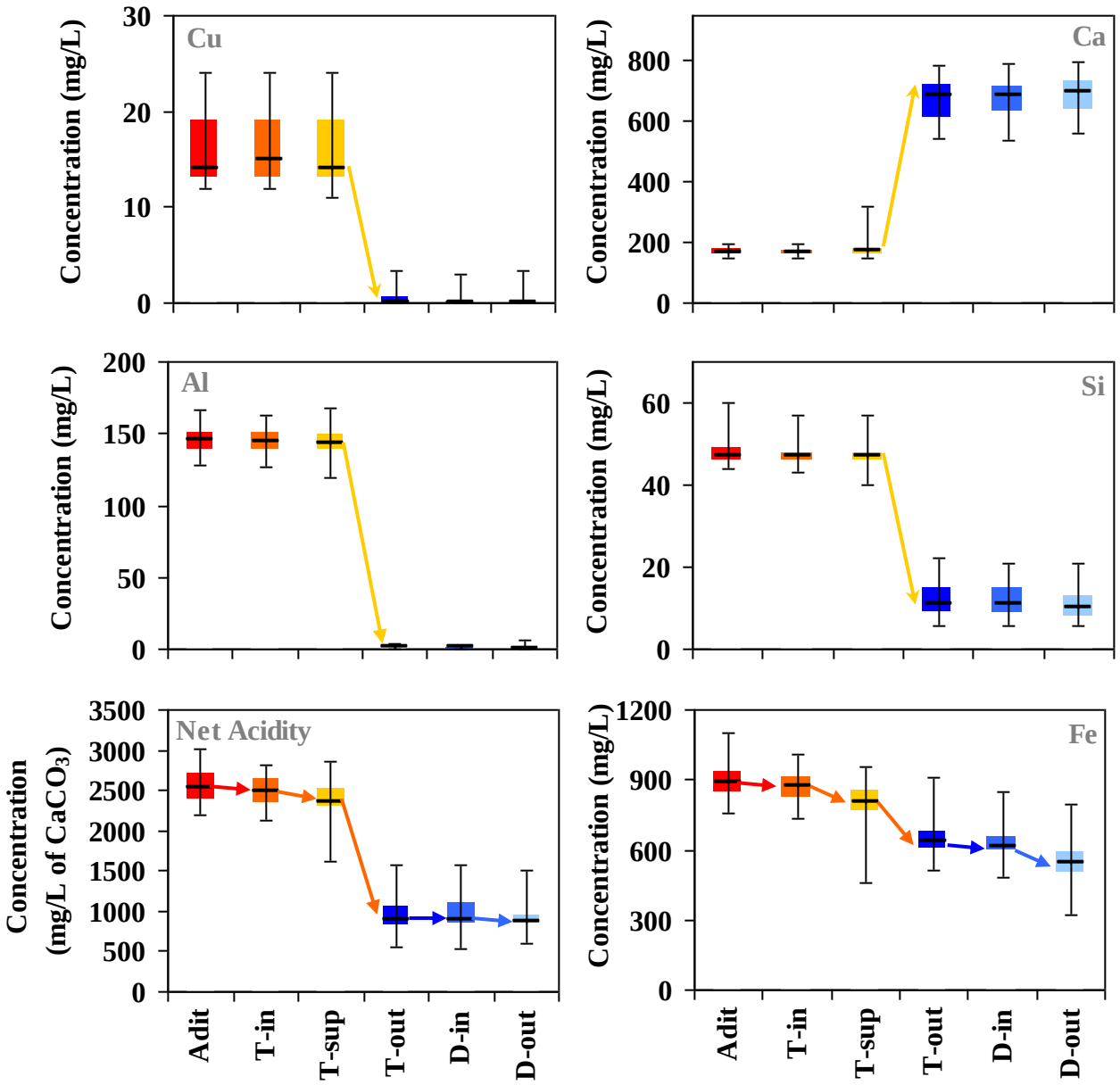
Cu
Concentration (mg/L)
30
20
10
0
Ca
Concentration (mg/L)
800
600
400
200
0
Al
Concentration (mg/L)
200
150
100
50
0
Si
Concentration (mg/L)
60
40
20
0
Net Acidity
Concentration (mg/L of CaCO3)
3500
3000
2500
2000
1500
1000
500
0
Fe
Concentration (mg/L)
1200
900
600
300
0
Adit
T-in
T-sup
T-out
D-in
D-out

Figure

Fig. 4

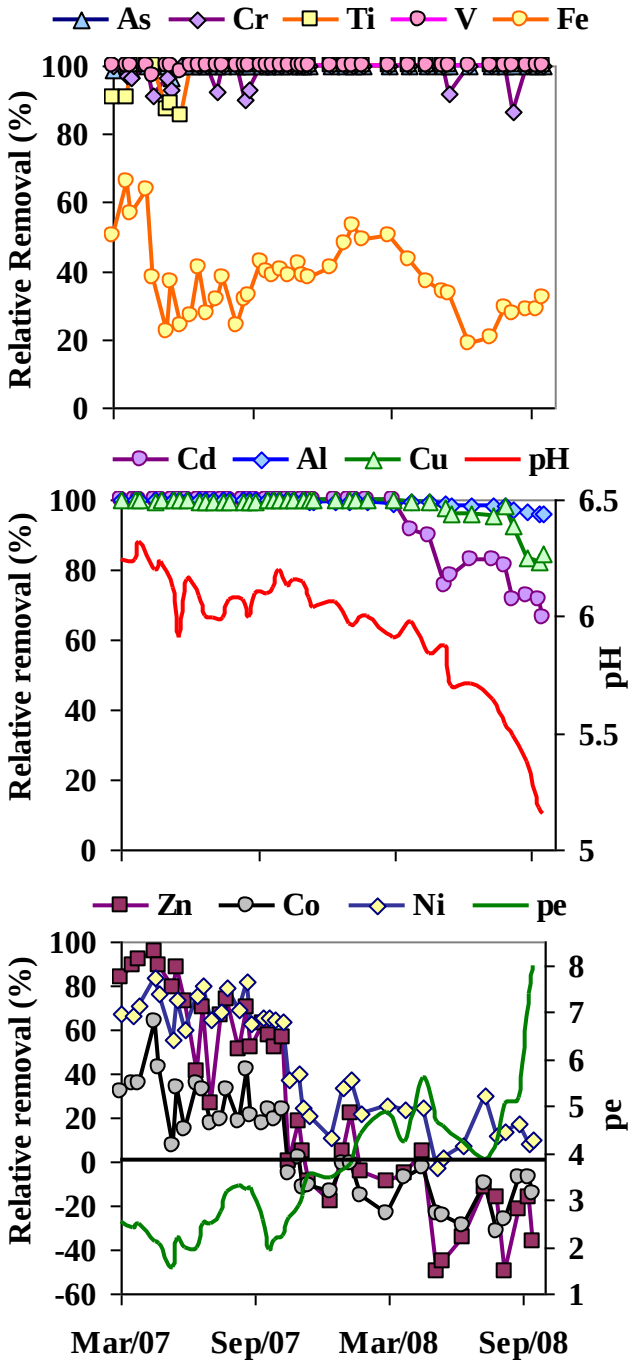
As
Cr
Ti
V
Fe
Relative Removal (%)
100
80
60
40
20
0
Cd
Al
Cu
pH
Relative removal (%)
6.5
6
5.5
5
Zn
Co
Ni
pe
8
7
6
5
4
3
2
1
-20
-40
-60
Mar/07
Sep/07
Mar/08
Sep/08

Figure

Fig. 5

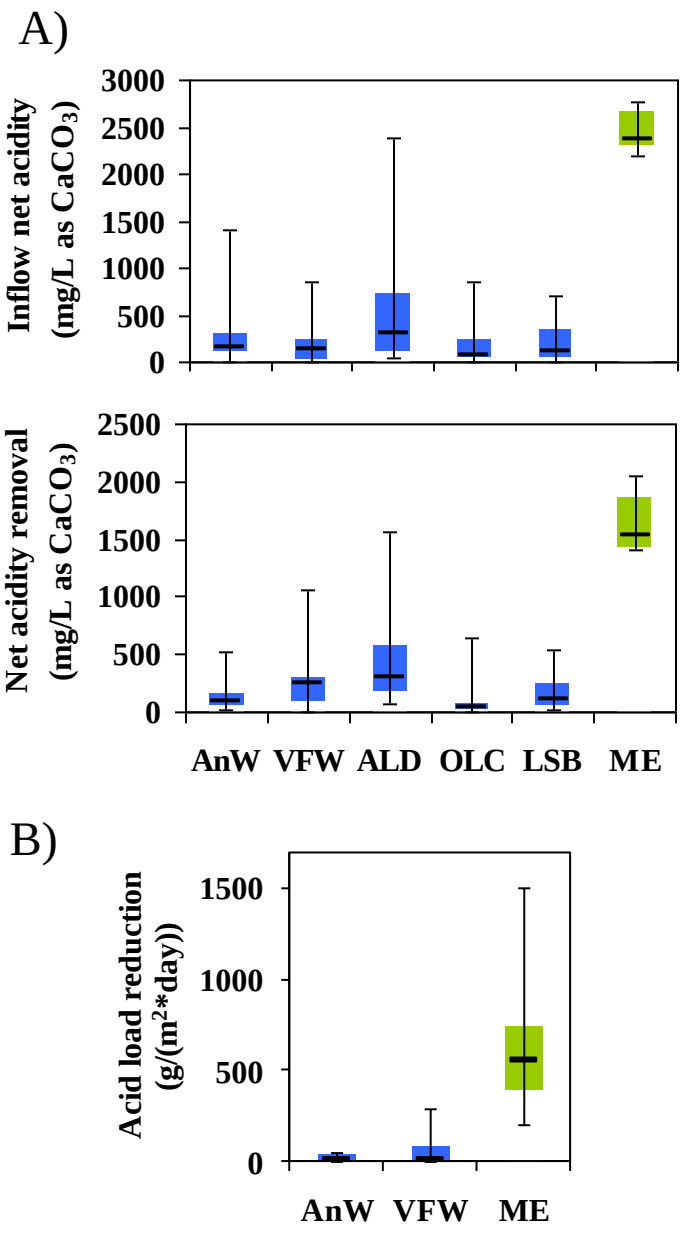
A)
Inflow net acidity (mg/L as $CaCO_3$)
3000
2500
2000
1500
1000
500
0
Net acidity removal (mg/L as $CaCO_3$)
2500
2000
1500
1000
500
0
AnW VFW ALD OLC LSB ME
B)
Acid load reduction (g/(m^2*day))
1500
1000
500
0
AnW VFW ME